International Conference on Space Optics—ICSO 2022

Dubrovnik, Croatia

3–7 October 2022

Edited by Kyriaki Minoglou, Nikos Karafolas, and Bruno Cugny,

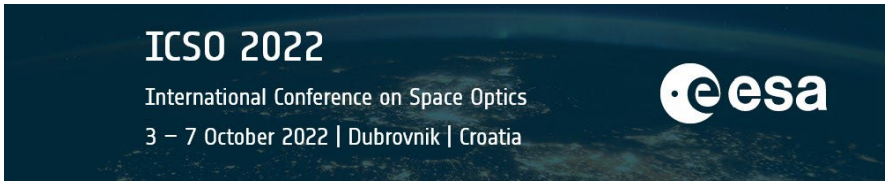

PROBA3-ASPIICS Coronagraph - Alignment, Performance Tests and Calibration

International Conference on Space Optics — ICSO 2022, edited by Kyriaki Minoglou, Nikos Karafolas, Bruno Cugny, Proc. of SPIE Vol. 12777, 1277767 · © 2023 ESA and CNES · 0277-786X · doi: 10.1117/12.2691118

PROBA3-ASPIICS Coronagraph - Alignment, Performance Tests and Calibration

Galy C*[a], Thizy C[a], Versluys J[b], Baeke A[a], Mazzoli A[a], Capobianco G[c], Fineschi S[c], Loreggia D[c], Zangrili L[c], Melich R[d], Leanerts C[a], Fleury-Frenette K[a], Jacobs J[a]
[a]CSL - Centre Spatial De Liège, Angleur, Belgium
[b]ESA - European Space Agency, Noordwijk, Netherlands
[c]INAF - Istituto Nazionale di AstroFisica, Torino, Italy
[d]IPP - TOPTEC, Turnov, Czech Republic

ABSTRACT

PROBA-3 is a mission devoted to the in-orbit demonstration (IOD) of precise formation flying (F^2) techniques and technologies for future ESA missions. The mission includes two spacecrafts. One of them will act as an external occulter for scientific observations of the solar corona from the other spacecraft, which will hold the ASPIICS coronagraph instrument, under CSL (Centre Spatial de Liège) responsibility.

The ASPIICS instrument on PROBA-3 looks at the solar corona through a refractive telescope, able to select 3 different spectral bands: Fe XIV line @ 530.4nm, He I D3 line @587.7nm, and the white-light spectral band [540;570nm]. The external occulter being located at ~ 150 meters from the instrument entrance, will allow ASPIICS to observe the corona really close to the solar limb, probably closer than any internally or externally occulted coronagraph ever observed.

CSL is responsible for the optical design, integration, testing and validation of the complete ASPIICS instrument.

The instrument qualification model (QM) underwent a full qualification campaign at CSL, providing confidence and assuring the performances of the coronagraph design. During the year 2021, the flight model (FM) was also successfully integrated and tested at CSL. The calibration performed at INAF during September 2021 was the last step to achieve before the instrument delivery to ESA end of 2021.

This paper will present the results of the qualification campaign, the optical performances of the flight instrument and the calibration campaign. Several challenges were faced during these campaigns, amongst which are detailed the alignment of the focal plane, the alignment measurement during environmental testing and setup constraints during the calibration. The successful validation of the instrument and its final acceptance is demonstrated.

Keywords: PROBA3, ASPIICS, Coronagraph, Alignment, Calibration, Telescope, Optical, Formation-flying

1 INTRODUCTION

PROBA-3 is a mission devoted to the in-orbit demonstration (IOD) of precise formation flying (F^2) techniques and technologies for future ESA missions. It is part of the overall ESA IOD strategy and it is implemented by the Directorate of Technical and Quality management (D/TEC) under a dedicated element of the General Support Technology Program (GSTP). The evolution of the design and achievements are presented in [3],[4],[6] and [7].

PROBA-3 will host ASPIICS (Association of Spacecraft for Polarimetric and Imaging Investigation of the Corona of the Sun) as primary payload, making use of the formation flying technique to form a giant coronagraph capable of producing a nearly perfect eclipse allowing observing the sun corona closer to the rim than ever before. The coronagraph system is distributed over two satellites flying in formation (approx. 150m apart). The so called Coronagraph SpaceCraft (CSC) carries the camera and the so called Occulter SpaceCraft (OSC) carries the sun occulter disc.

A secondary payload will be embarked on the occulter satellite; it consists of the DARA solar radiometer.

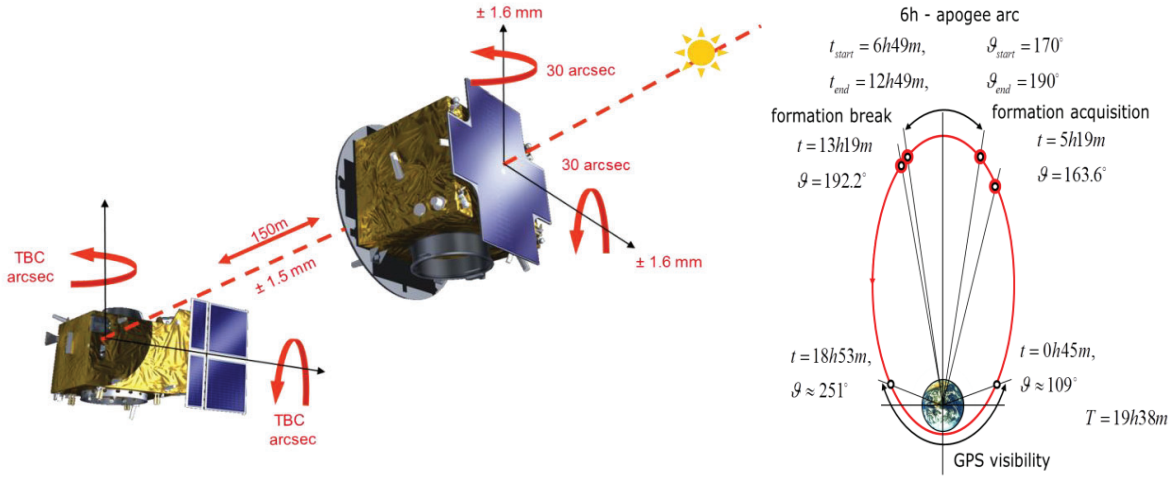

Figure 1. PROBA-3 formation flying overview and orbit.

The science objectives of the mission are presented in [1] and [2]. These are basically the observation of the solar corona in an area close to 1 solar radius, where the magnetic field plays a crucial role in the coronal dynamics, thus providing continuous observational conditions very close to those during a total solar eclipse, but without the effects of the Earth's atmosphere.

The proposed PROBA-3 Coronagraph System (ASPIICS) will be the first space coronagraph to cover the range of radial distances between 1.1 and 3 solar radii. ASPIICS will combine observations of the corona in white light and polarization brightness with images of prominences in the He I 5877 Å line and in the Fe XIV 5304 Å line.

ASPIICS will provide novel solar observations to achieve the two major solar physics science objectives: to understand physical processes that govern the quiescent solar corona, and to understand physical processes that lead to coronal mass ejections (CMEs) and determine space weather.

The PROBA-3 coronagraph optical design follows the general principles of a classical externally occulted Lyot coronagraph. The external occulter (EO), hosted by the Occulter Spacecraft (OSC), blocks the light from the solar disc while the coronal light passes through the circular entrance aperture of the Coronagraph Optical Box (COB), accommodated on the Coronagraph Spacecraft (CSC).

The optical model of ASPIICS and its predicted performances are presented in [5]. The optical design and its main elements are illustrated in Figure 2 below. The telescope is an all-refractive optical design with lenses and barrel manufactured by TOPTEC - Institute of Plasma Physics in Czech Republic.

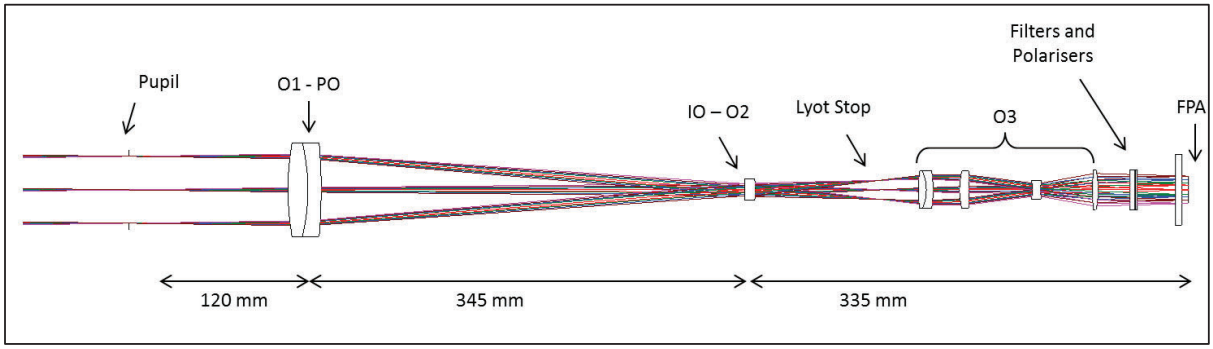

Figure 2. Optical design model of ASPIICS

Figure 3 below illustrates the straylight model of the coronagraph instrument elaborated at CSL for a straylight analysis which was an important part of the theoretical validation of the design. This analysis is presented in detail in [8].

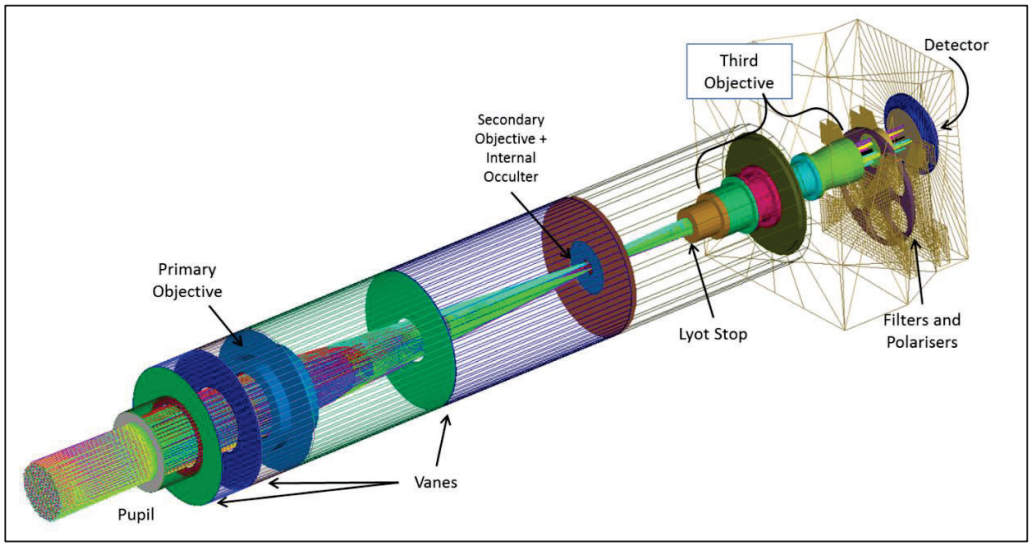

Figure 3. Straylight model of ASPIICS

In October 2019, the Qualification Model (QM) of the Coronagraph Instrument (CI) was integrated at CSL. This was the beginning of the first optical performance testing campaign performed on the complete instrument. During this campaign, different procedures and setups were tested to qualify the optical performances of the ASPIICS Coronagraph. The alignment setup demonstrated its efficiency, and the results will be presented below. The verification of the optical performances mainly consisted in the verification of the Point Spread Function (PSF) of the CI. An optomechanical setup using a collimator together with a hexapod was the key to a successful validation of these performances. Finally, all the alignment and test equipment are designed for ASPIICS operational environment, allowing an easy follow-up of the performances during environmental testing.

After a successful qualification campaign, the Flight Model (FM) of the instrument is fully integrated, aligned and tested at CSL between September 2020 and June 2021. Most of the optical alignment and performances verification are performed again to confirm the instrument acceptance before calibration of its optical behavior.

The calibration campaign took place at INAF during the month of September 2021. During this campaign, the instrument is submitted to several tests in ambient and operational environment which aimed to provide calibration references and key data parameters regarding the radiometric, spectral and polarization behavior of the instrument. These data will then serve to properly process the scientific images during the operation period of the spacecraft, and will be compared to in-flight calibration data.

2 QUALIFICATION MODEL ALIGNMENT AND TEST

During the design phase of the coronagraph instrument, the tolerance analysis considered two alignment parameters. These parameters - called “compensators” - were defined as the focus (longitudinal) positioning of two elements. The first element is the Primary Objective (PO) performing an image of the sun onto the internal occulter (cf. Figure 2 “IO-O2”). This internal occulter is a black coating deposited onto the flat front surface of the second objective lens (“O2”), designed and performed at CSL.

The second and major compensator element is the focus position of the Focal Plane Assembly (FPA).

The main objective of the alignment test is to define a correct location for the two elements with the help of specifically manufactured shims to be inserted at their interface with the mechanical structure. The mechanical design of the coronagraph structure considered a reference shim thickness for both locations. The thickness of this shim can then be reduced or increased depending on the alignment test output.

The problematic of this alignment lies within the fact that the coronagraph is meant to be operated in environmental conditions (temperature, pressure) that are quite different from the ground test environment. In the same time, it shall also be possible to operate the instrument at ambient temperature and in air to verify its performances.

It is therefore necessary to define two alignment configurations as described below in Table 1.

Table 1. Alignment environmental configuration

Configuration	Environment	CI Temperature	PO Compensator	FPA Compensator
Ground test	Air	20°C	PO_Shim$_{AIR}$	FPA_Shim$_{AIR}$
Operational	Vacuum	35°C	PO_Shim$_{OP}$	FPA_Shim$_{OP}$

The PO shim thickness was defined considering the real measurement of all parameters on the QM optical design: lenses radius of curvature, decentering, refractive index. The subsystem PO-Internal occulter being simple enough to evaluate the shim thickness, a thermoelastic analysis provides the necessary inputs to estimate its value in operational condition with a minimal error.

Concerning the FPA shim thickness, it was first foreseen to be estimated in the same way. Due to the complexity of the thermoelastic impact on the whole instrument the plan changed during the critical design phase and a more efficient setup was designed and is presented below.

2.1 Alignment setup and facility

A great improvement in the estimation of the final shim thickness is reached with the definition of a dedicated alignment setup to mount the focal plane of the instrument at the right location in both configurations. This setup consists first in the dissociation of the focal plane assembly from the rest of the instrument. This allows an easy translation during the test campaign. A dedicated mechanical interface is designed to hold the instrument FPA instead of the equipment box (cf. picture in Figure 4 below).

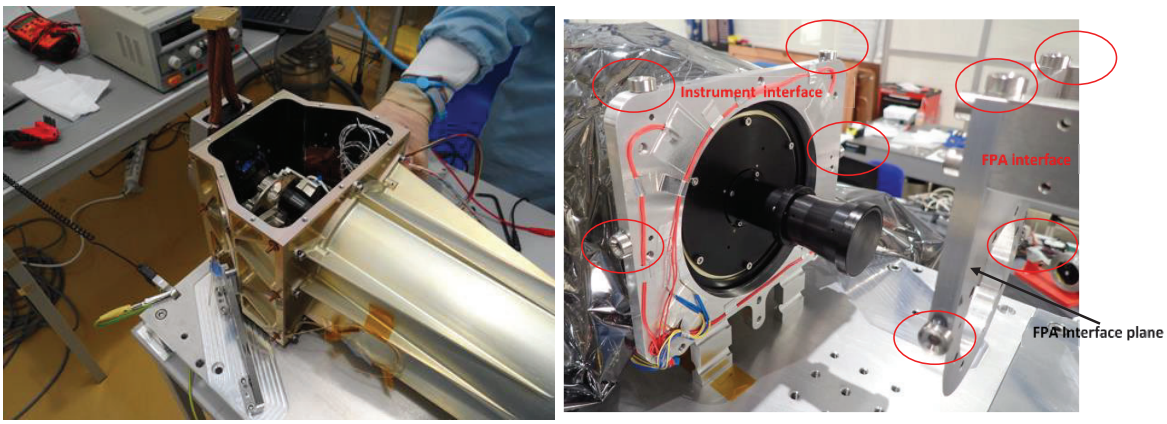

Figure 4. Assembled (left) and dissociated (right) FPA from the equipment box (EQB)

Another mechanical interface is also defined to hold the instrument tube, as illustrated above. Both interfaces are equipped with laser tracker targets to ease and control the alignment between them, and to be able to report the correct distance needed for the FPA focus position.

In that configuration, the filter wheel assembly inside the EQB is also removed. The optical properties of the missing filters need to be taken into account for the final estimation of the shim thickness.

The FPA mechanical interface is mounted onto a small hexapod, providing enough translation and rotation range to cover the shim thickness allowable range and the alignment of both interface plates. The design and the actual setup are presented below in Figure 5.

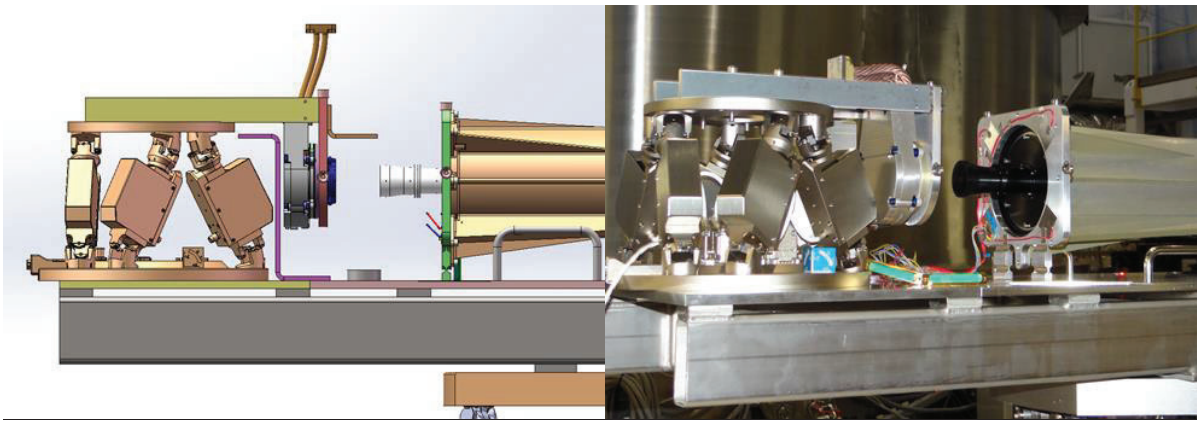

Figure 5. CAD (left) and actual (right) FPA alignment setup close-up

The whole set-up including the instrument is finally mounted on a larger hexapod inside a thermal vacuum chamber connected to an appendix hosting a collimator. This collimator is designed to illuminate the instrument with different angular patterns depending on the test to be conducted. The mechanical design and the real setup are illustrated in Figure 6 below.

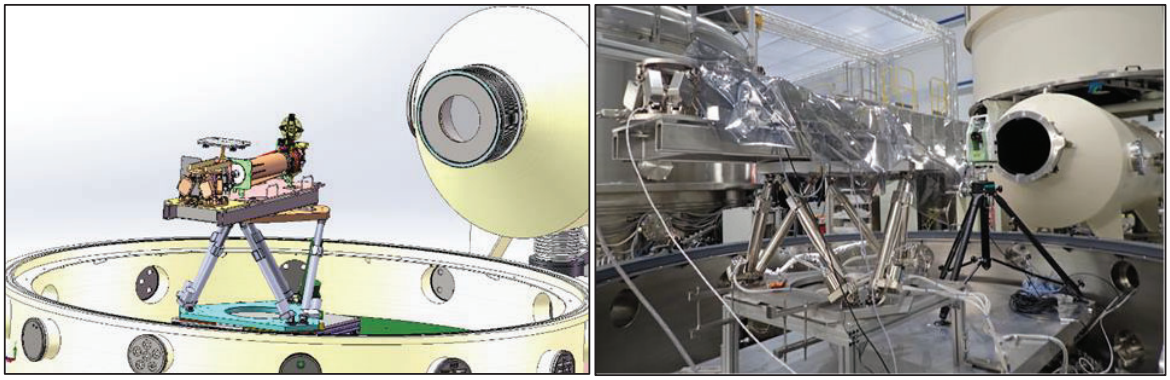

Figure 6. CAD (left) and actual (right) alignment setup inside the vacuum chamber

This vacuum chamber can be closed and the pressure can be controlled down to $<10^{-5}$ mbar, allowing the tests to be performed either in air or in vacuum. In addition, the instrument is equipped with thermal heaters that can be operated to stabilize the instrument at operational temperature.

2.2 Alignment and performances in air

For the alignment test sequence, two different configurations of the collimator are defined. The first configuration is a small pinhole at the focal plane of the collimator providing an illumination at the instrument FPA designed to be spread across a maximum of two pixels squared. This was defined considering a diffraction limit of ~19.4µm and a pixel size of 10 µm. By translating the instrument focal plane along the longitudinal direction, the acquisition of the resulting spot images along the way provides sufficient input to define the best focus position. This best focus is the location of the FPA where the spot radius is the smallest. A centroidisation algorithm along with the determination of the associated RMS radius then gives a best-focus search curve of the RMS spot radius versus the focus position.

This curve should theoretically have a minimum and unique best focus as well as a linear behavior down to ½ pixel. In reality the diffraction limit of the instrument and the spatial extend of the spot create a more "rounded" behavior close to the best focus location. A linear fit of the curve farther before and after the estimated best focus shows then both lines crossing at the actual best focus location. Figure 7 below shows a simulation of the alignment with a perfect instrument and the associated result in air with the QM instrument. The associated FPA_Shim$_{AIR}$ thickness is then computed considering this best focus location and several other parameters as defined below.

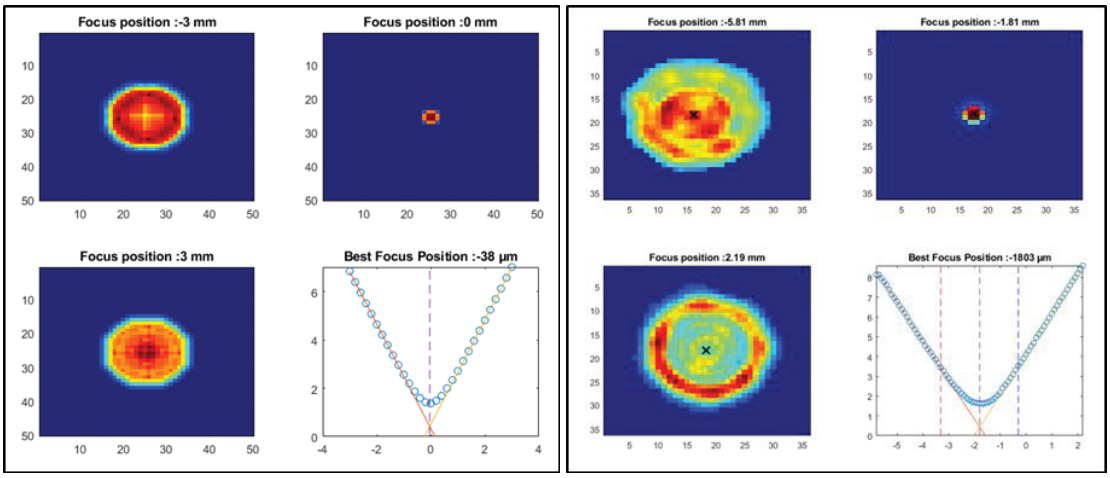

Figure 7. Best focus search simulation (left) and result in air (right)

The shim thickness is assessed considering the following parameters and equation (1):

Initial EQB length (L_{EQB}), measured distance between interfaces (D_{IF}), defocus introduced by the filters (D_{Filter}), initial (X_0) and best focus (X_{BF}) position of the hexapod.

$$FPA_{Shim_{AIR}} = D_{IF} + (X_0 - X_{BF}) + D_{Filter} - L_{EQB} \quad (1)$$

In order to verify the performances of the instrument at the best focus, another configuration of the collimator setup is used. This time, the focal plane is equipped with very thin slits (image width < 0.4 pixels). The collimator illuminates the instrument with a slit pattern, and this pattern is translated at the focal plane with a step of 0.2 pixel. Those values are considered in accordance with the fact that the diffraction limit of the instrument spreads on two pixels.

The acquisition of images during the translation provides inputs for a Point Spread Function (PSF) computation. The Full width at Half Maximum (FWMH) of this retrieved PSF defines the performance of the instrument. In our case, this test is performed once after the best focus search by placing the detector at the best focus location. After that, the associated FPA_Shim_{AIR} is manufactured and the FPA is mounted back on the EQB. The PSF test is performed again to compare the results and validate the thickness evaluation of the FPA_Shim_{AIR} and the re-integration of the complete instrument. Figure 8 below shows the almost identical comparison between the PSF measured on the alignment setup and the PSF measured after complete integration with the shim.

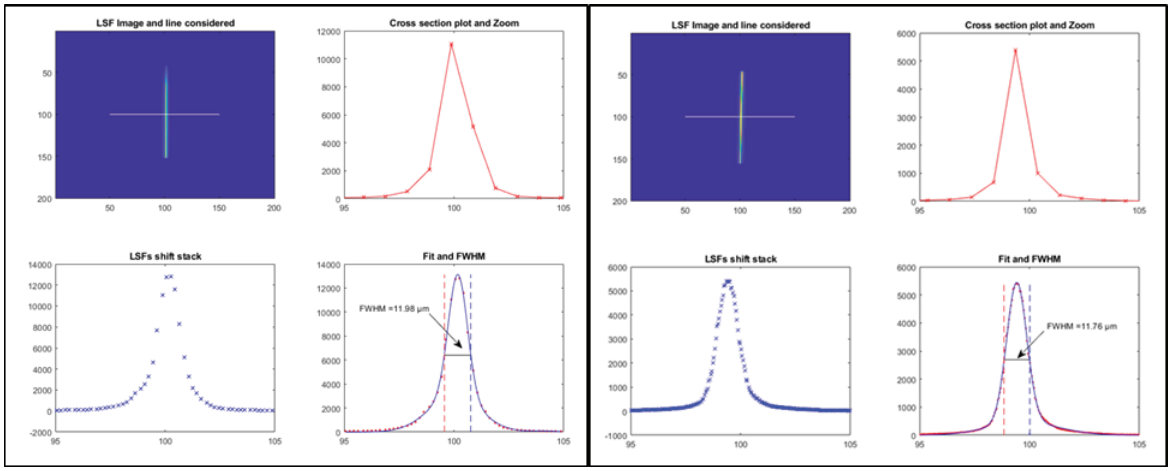

Figure 8. PSF in air, at best focus on hexapod (left) and with ambient shim mounted (right)

2.3 Alignment and performances under operational conditions

The alignment test and the performance verification of the QM instrument is performed once again, this time under operational environment. The PO_Shim$_{AIR}$ is replaced by the PO_Shim$_{VAC}$, and the FPA is put back on the alignment setup interface after disassembling the EQB.

In order to perform this test under operational conditions, the instrument is covered with multi-layer insulation (MLI) sheets, thermocouples are installed at different locations around the instrument to monitor the thermal behavior and the vacuum chamber is closed. Once the vacuum condition is reached, the instrument heaters are controlled to raise the temperature to the operational value (35°C). Once stabilized, the same procedure as in air is applied to define the best focus location and verify the PSF performances.

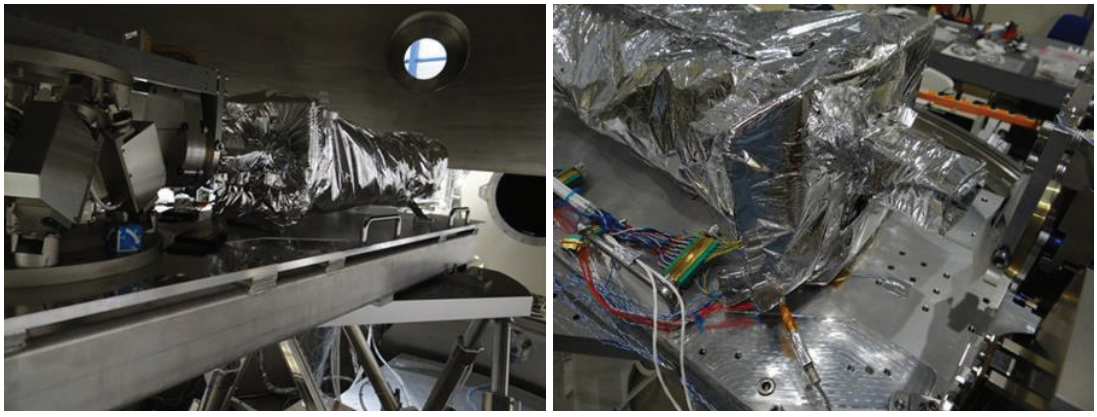

Figure 9. Instrument wrapped in MLI inside TVAC chamber (left) and alignement setup close-up (right)

Figure 9 above shows the vacuum configuration of the test with the MLI-covered instrument. For this test, the environment surrounding the instrument is not controlled to an operational thermal environment. Figure 10 below presents the best focus search results and the PSF verification with the instrument FPA on its alignment setup. For the PSF measurement, the steps were reduced to ~1/10th of the estimated PSF FWHM to provide a better accuracy of the curve retrieval.

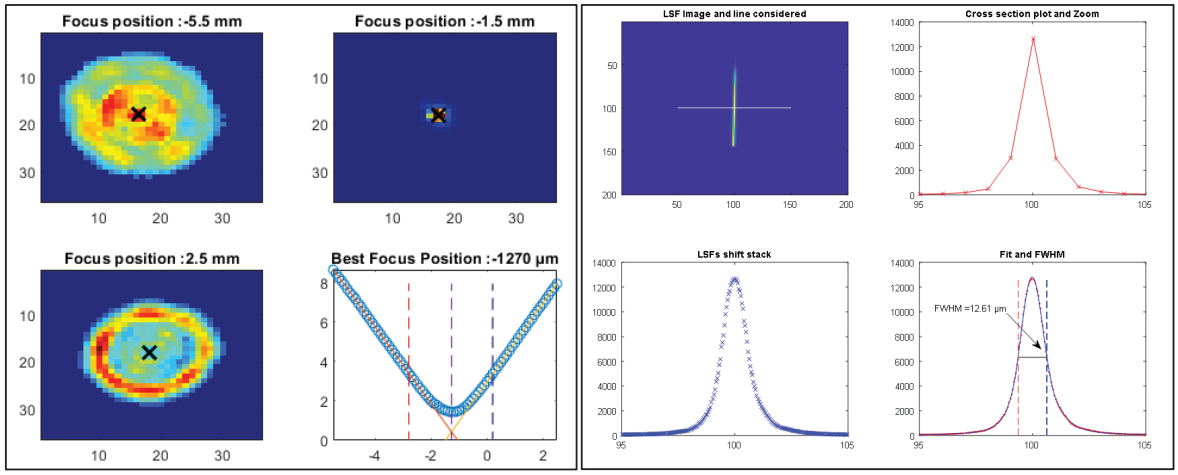

Figure 10. Best focus search and PSF performance in operational environment

As presented above, the best focus search leads to a quite different best focus location. The aspect was already estimated, and is mainly due to the fact that the optical design includes many refractive elements whose refractive indexes and geometrical properties are sensitive to the temperature and the pressure change. Although estimated, the result showed a slight difference with the predicted change. This justifies and confirms the need to actively compensate the system before defining the final shimming.

2.4 QM optical performance conclusion

During this performance test campaign, the alignment procedure provided a full compliance of the instrument performances in air by showing a compliant PSF measurement at best focus position and after integration of the final shims. This compliance induced a confidence in the measurement procedure and in the shim final estimation, showing that the remaining uncertainties are covered by the final shim computation method. Even when no PSF verification were performed on the final instrument under operational condition, the procedure is validated and the final performances are considered in line with the performance requirements.

During this qualification test campaign, lots of other performances tests were performed and will not be presented here. For instance, the instrument features a small diffuser at the center of the front door assembly. Its aim is to provide a flat field illumination on the detector when illuminated by a sun-like source. This diffuser is characterized and verified during the test campaign (homogeneity and required attenuation) using a high power laser diode as source for the collimator setup. This high power laser diode setup was also used to validate the straylight model presented in [8].

Finally, the QM campaign also aimed to qualify the structural behavior of the instrument to vibration and temperature excursion. A specific test setup is defined with theodolites to measure the relative orientation of several alignment cubes on the CI structure along with the line of sight of the instrument. These parameters are measured before and after each vibration or thermal vacuum test to confirm the structural stability of the instrument.

3 FLIGHT MODEL PERFORMANCES

The flight model integration started end of November 2020 and the test campaign was held at CSL between November 2020 and April 2021. Some changes were made with respect to the QM test campaign. It mainly consisted in a vacuum chamber change for the alignment and performance testing due to programmatic constraints. This resulted in a necessity to redefine the alignment setup and operation. The collimator test setup was removed from the previous chamber and directly inserted in the new vacuum chamber along with the instrument and alignment test setup. Figure 11 below illustrates the FM instrument test configuration in the new vacuum chamber. The pictures also show the collimator setup which was removed from the previous chamber appendix.

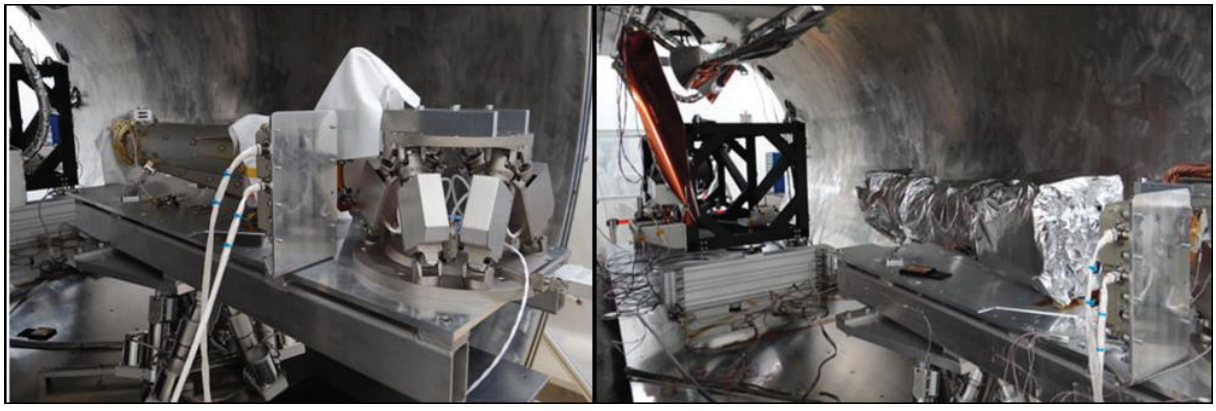

Figure 11: FM instrument, alignment setup and collimator in the chamber for air (left) and vacuum (right) performance tests

The alignment and performance tests are conducted following the procedure of the QM campaign. During ambient performance tests, only a verification of the procedure was performed to give confidence in the alignment setup. The best focus search at ambient and the PSF measurement at best focus are considered, but the instrument was missing some FM elements (mainly FM FPA). Due to additional integration constraints on the FM model, it was also decided to directly integrate the PO_Shim_{VAC} instead of the PO_Shim_{AIR} to limit the amount of integration operations. The complete FM instrument was available for the operational testing phase, during which both performance tests were conducted. The final verification of the integrated instrument performances is performed at this level. Several additional operational verifications including performances across the field of view and temperature sensitivity are conducted during this phase to completely confirm the instrument performances.

3.1 Alignment and performances in air

The best focus search of the FM alignment in ambient condition is presented in Figure 12 below. As for the QM alignment, the best focus position is determined by scanning the focus position of the FPA with the alignment hexapod while looking at the pinhole through the collimator. Figure 12 below presents the best focus search result.

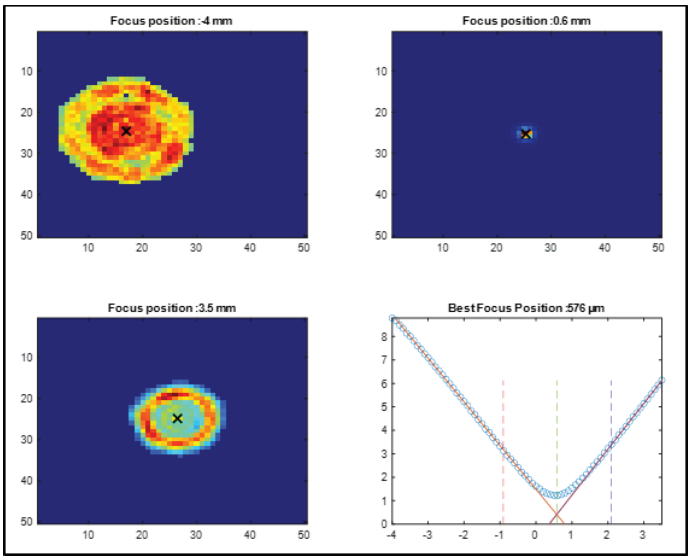

Figure 12. Best focus search result in air

As previously mentioned, this test aimed to verify the alignment procedure. The final shim thickness is not computed, but the PSF verification is performed at the defined best focus location as illustrated in Figure 13 below.

For the FM alignment, the PSF FWHM is now compared with a theoretical value considering the nominal instrument diffraction limit (~19.36µm), the pixel width (10µm) and the test setup optical properties. An uncertainty of ±1µm is estimated on the computation and an error of ±0.5µm is estimated on the measurement. Figure 13 below shows the PSF verification results and the good match between the theoretical and measured PSF.

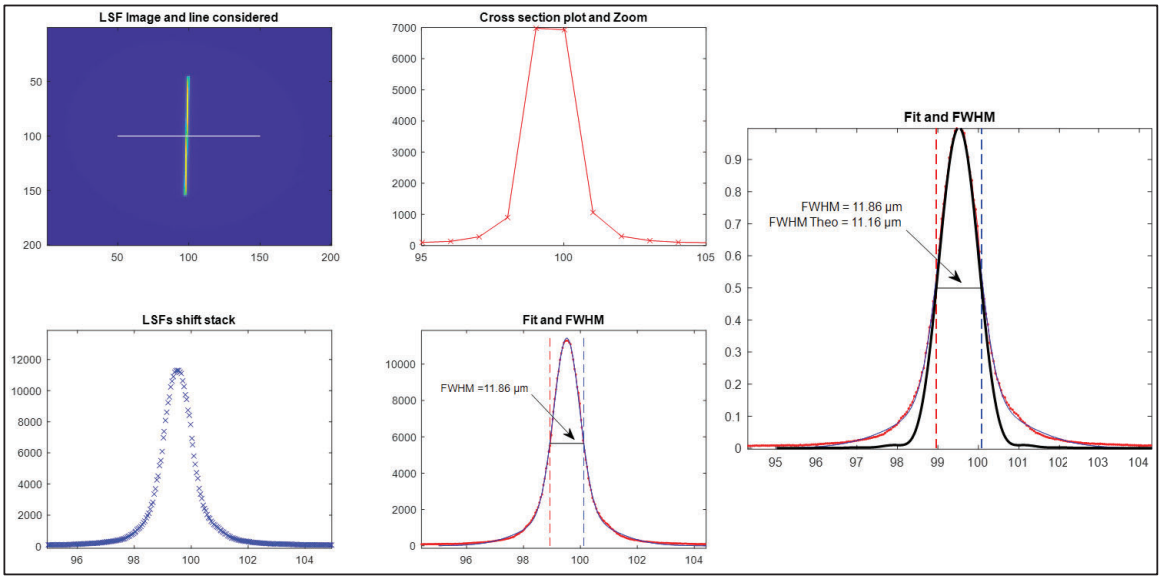

Figure 13. PSF performances at best focus, in air

3.2 Alignment and performances under operational conditions

The instrument is then aligned in operational environment, i.e. under vacuum and thermally stabilized at 35°C ± 1.5°C. At this stage, the EQB and the filter wheel assembly are still not mounted onto the instrument in order to be able to perform the best focus search procedure under vacuum. The plan is then to define the operational FPA_Shim$_{VAC}$, and to manufacture it for final integration and verification of the complete instrument.

The instrument is set up with various thermocouples to monitor and control the temperature at different locations and to ensure a good stabilization at the required operational temperature. Figure 14 below shows the best focus search during this operational test. The different temperatures on the instrument are also reported.

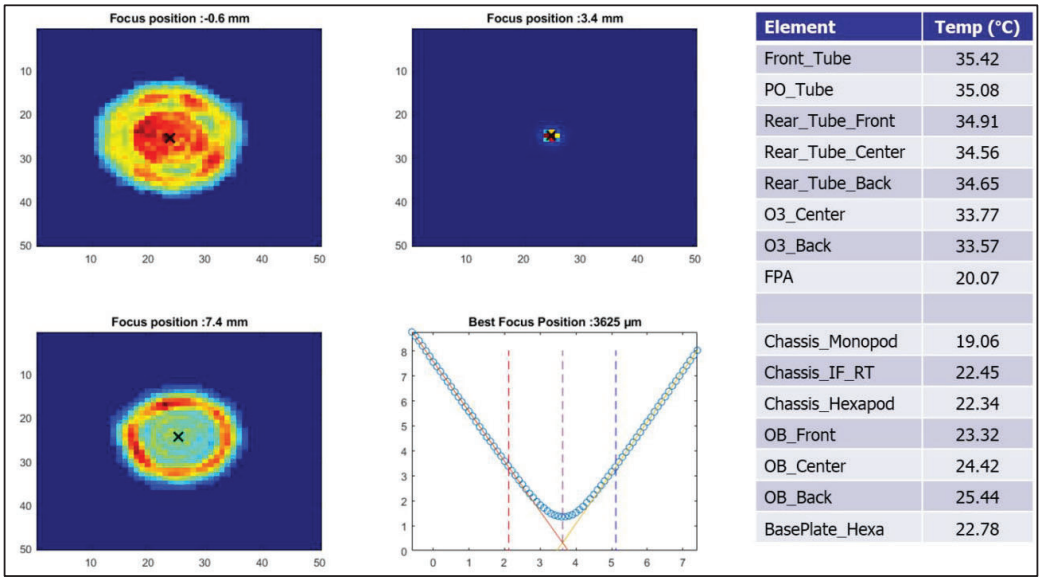

Element	Temp (°C)
Front_Tube	35.42
PO_Tube	35.08
Rear_Tube_Front	34.91
Rear_Tube_Center	34.56
Rear_Tube_Back	34.65
O3_Center	33.77
O3_Back	33.57
FPA	20.07
Chassis_Monopod	19.06
Chassis_IF_RT	22.45
Chassis_Hexapod	22.34
OB_Front	23.32
OB_Center	24.42
OB_Back	25.44
BasePlate_Hexa	22.78

Figure 14. Best focus search results - Operational conditions

This best focus search is successfully performed and the final shim thickness can be computed using the same method as shown in equation (1) for QM campaign. An additional thermal contribution of the alignment setup however needs to be taken into account considering the structural difference between the alignment setup configuration and the final operational instrument. This contribution considered the measured temperature of the optical bench during the alignment test and the thermoelastic deformation difference between the optical bench and the EQB at operational temperature.

In the end, the final FPA_Shim$_{VAC}$ is computed following equation (2) and the parameters below:

$$FPA_{Shim_{VAC}} = D_{IF} - (X_{BF} - X_0) + IF_{shim} + D_{Filter} - L_{EQB} - Dth_{FPA} \quad (2)$$

D_{IF} : Initial measured distance between FPA and CI interfaces at best ambient focus position

X_{BFP} : Hexapod position at best operational focus

X_0 : Initial hexapod position at best ambient focus

IF_{Shim} : Thickness of the shim between FPA and its interface

D_{Filter} : Additional defocus introduced by the FM filters

L_{EQB} : Measured length of the FM EQB

Dth_{FPA} : Additional thermal deformation induced by the structural difference between alignment and mounted CI

The final shim thickness could then be estimated from the operational alignment test.

Before starting the manufacturing of the final shim a verification is performed using the PSF measurement test. This verification is presented in Figure 15 below along with the temperature of the different elements.

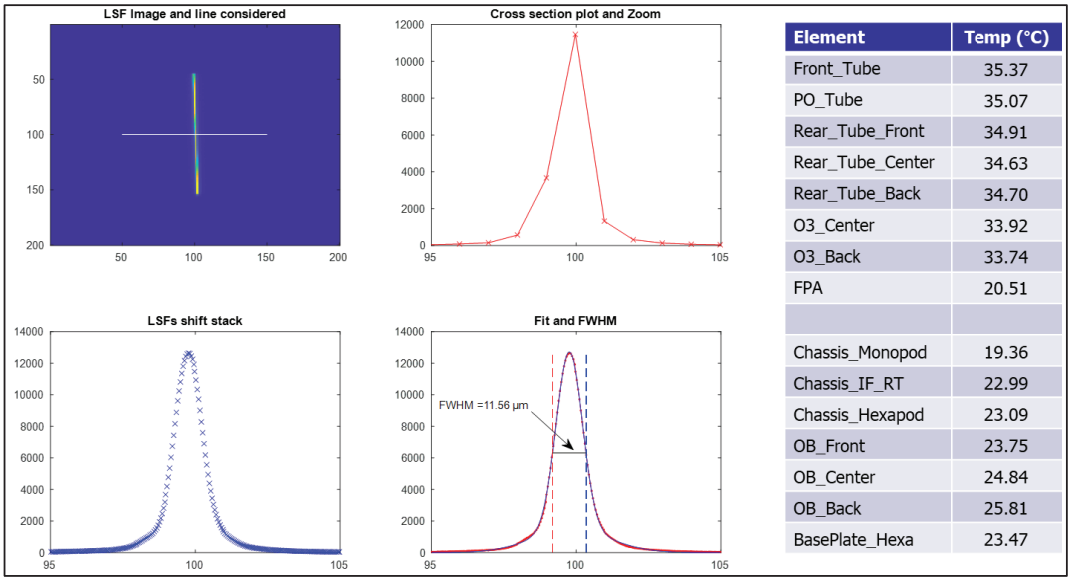

Element	Temp (°C)
Front_Tube	35.37
PO_Tube	35.07
Rear_Tube_Front	34.91
Rear_Tube_Center	34.63
Rear_Tube_Back	34.70
O3_Center	33.92
O3_Back	33.74
FPA	20.51
Chassis_Monopod	19.36
Chassis_IF_RT	22.99
Chassis_Hexapod	23.09
OB_Front	23.75
OB_Center	24.84
OB_Back	25.81
BasePlate_Hexa	23.47

Figure 15. PSF performance at best focus - Operational conditions

At this moment, two additional performance verifications are also performed. First, the instrument is heated up to 38°C. The FPA focus position is kept at best operational focus, and the PSF is measured. No visible degradation is observed compared to the PSF at 35°C. This test verified that the thermal sensitivity of the instrument can be considered negligible at 35 ±1.5°C. During the cooling down of the instrument a last PSF verification is also performed by slightly changing the FPA focus position by ±150µm. The results are presented in Figure 16 below and show a PSF FWHM increase by only 0.3µm through focus, which is considered negligible (~1.5% of the diffraction limit).

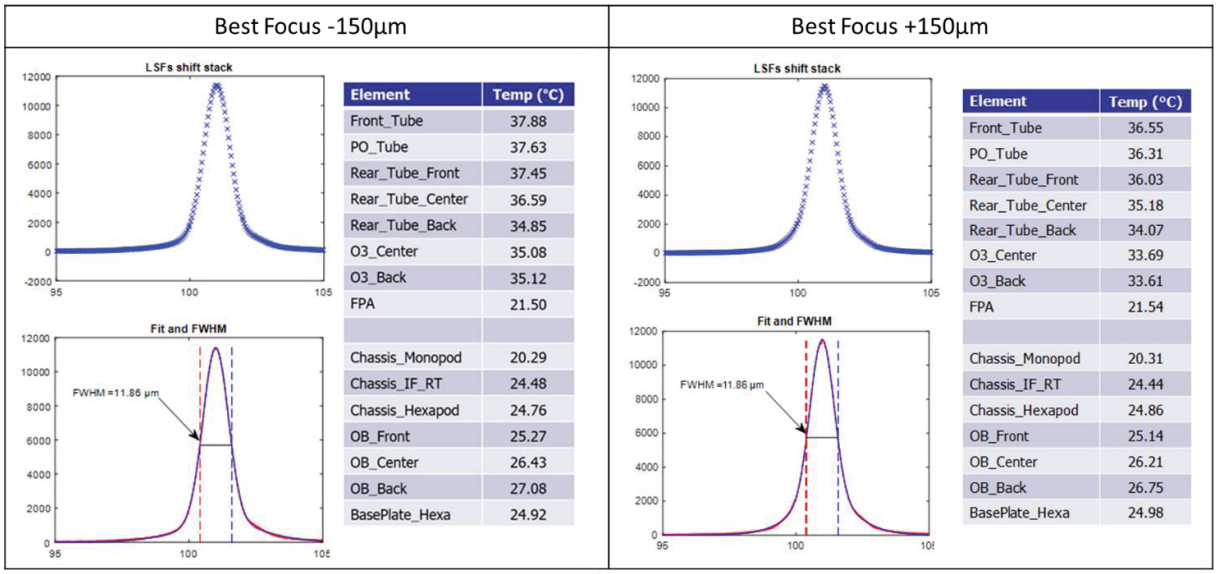

Element	Temp (°C)
Front_Tube	37.88
PO_Tube	37.63
Rear_Tube_Front	37.45
Rear_Tube_Center	36.59
Rear_Tube_Back	34.85
O3_Center	35.08
O3_Back	35.12
FPA	21.50
Chassis_Monopod	20.29
Chassis_IF_RT	24.48
Chassis_Hexapod	24.76
OB_Front	25.27
OB_Center	26.43
OB_Back	27.08
BasePlate_Hexa	24.92

Element	Temp (°C)
Front_Tube	36.55
PO_Tube	36.31
Rear_Tube_Front	36.03
Rear_Tube_Center	35.18
Rear_Tube_Back	34.07
O3_Center	33.69
O3_Back	33.61
FPA	21.54
Chassis_Monopod	20.31
Chassis_IF_RT	24.44
Chassis_Hexapod	24.86
OB_Front	25.14
OB_Center	26.21
OB_Back	26.75
BasePlate_Hexa	24.98

Figure 16: Through focus PSF verification

These two additional verifications confirmed the performance compliance of the FM instrument and its negligible sensitivity to temperature and defocus error.

The final shim is then manufactured and integrated in the FM instrument. The performance verification test now consists in a PSF verification for different configurations:

1. First PSF measurement at 32°C, then stabilization at 35°C
2. Measurement at center field of view (FoV) with all filters
3. Measurement at ±0.7° in both directions to confirm the performances in the FoV and verify the CI FoV.
4. Heating up to 38°C and last PSF measurement

The PSF performance of the instrument at center field of view is presented below in Figure 17.

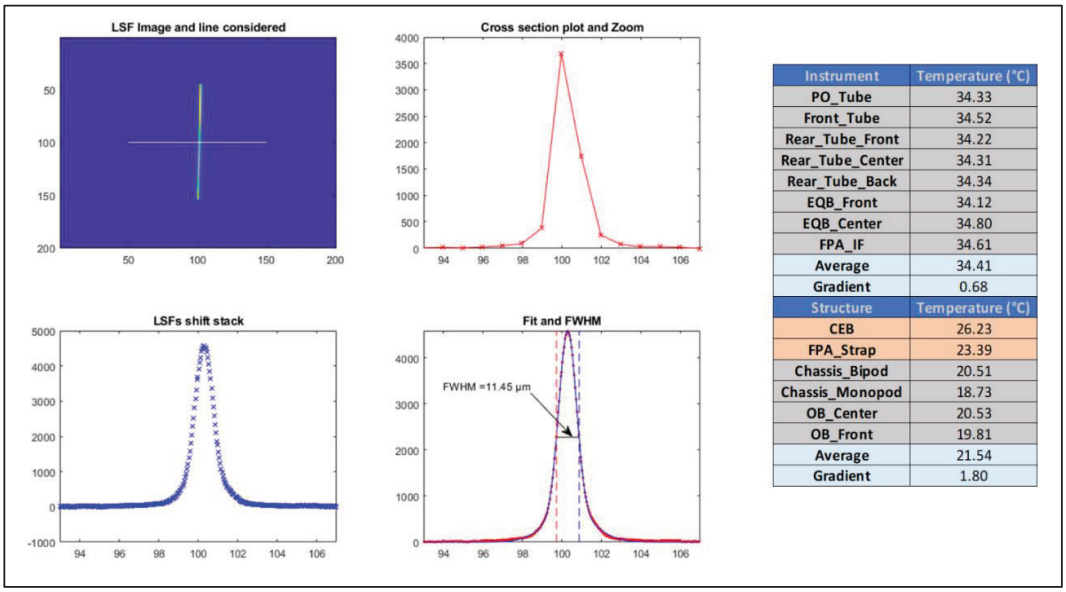

Instrument	Temperature (°C)
PO_Tube	34.33
Front_Tube	34.52
Rear_Tube_Front	34.22
Rear_Tube_Center	34.31
Rear_Tube_Back	34.34
EQB_Front	34.12
EQB_Center	34.80
FPA_IF	34.61
Average	34.41
Gradient	0.68
Structure	**Temperature (°C)**
CEB	26.23
FPA_Strap	23.39
Chassis_Bipod	20.51
Chassis_Monopod	18.73
OB_Center	20.53
OB_Front	19.81
Average	21.54
Gradient	1.80

Figure 17. PSF Performance with Wide Band Filter (WBF), final mounted shim and operational conditions

Table 2 below summarizes the PSF performance results for all the configurations. The instrument field of view (FoV) was measured by applying a centroidisation algorithm on the PSF images performed at ±0.7° in horizontal and vertical direction to retrieve the pixel span corresponding to 1.4°. Extrapolating to the 2048-pixels width gives the complete FoV.

Table 2. Final performance verification of FM under operational conditions

FoV Rz (°)	FoV Ry (°)	Temp (°C)	Filter	PSF FWHM (µm)	Specification
0	0	32	WBF	12.43	N/A
0	0	35	WBF	11.45	PSF FWHM ≈11.16 ±1µm
0.7	0	35	WBF	11.31	
-0.7	0	35	WBF	11.03	
0	0.7	35	WBF	11.31	
0	-0.7	35	WBF	11.59	
0	0	35	He I D3	12.01	
0	0	35	Fe XIV	10.75	
0	0	35	Pol #1	11.45	
0	0	35	Pol #2	11.17	
0	0	35	Pol #3	11.45	
0	0	38	WBF	11.03	N/A
Field of View				**Measured**	**Specification**
Horizontal Complete FoV				1.6036°	±0.8°
Vertical Complete FoV				1.6018°	±0.8°

3.3 FM optical performances conclusion

The alignment of the FM instrument has been successfully performed during the campaign between November 2020 and February 2021. An operational compensation shim is defined, and the optical performances of the coronagraph instrument are confirmed for all configurations.

Before starting the instrument calibration, the environmental testing of the instrument is conducted between February 2021 and June 2021 during which the FM instrument is subjected to thermal-vacuum and vibration tests at CSL. Functional tests on all the subsystems are performed during those tests. Additionally, the structural misalignment of the instrument is also measured before and after the environmental testing by controlling the relative orientation of reference cubes on the instrument, on the optical bench, and of the instrument line of sight materialized by the orientation of the internal occulter center. A quick example of the misalignment measurement setup is presented in Figure 18 below.

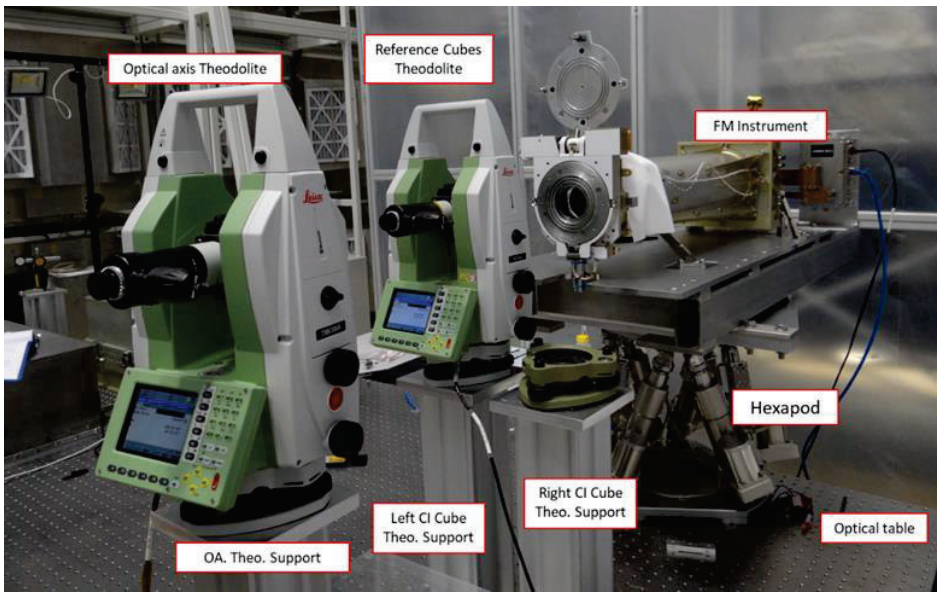

Figure 18: Instrument misalignment measurement setup

This setup is designed as a “plug-and-play” measurement setup where the instrument is simply put back to the same location and orientation on the setup before and after each test. This setup allowed accurate measurement and verification of the FM instrument structural misalignment during the whole environmental test campaign.

4 FLIGHT MODEL CALIBRATION

The final step of the FM instrument before delivery to the customer (ESA) is to perform a ground test calibration of its optical properties. The calibration campaign is designed to produce calibration images that will help the science team to link the measured electronic signal per pixel of each measurement to actual scientific data (i.e. number of protons, polarization, spectral behavior …) and to actively correct the acquired images.

The calibration campaign included a radiometric, spectral and polarization calibration of the optical instrument and its main features: High Density Diffuser (HDD) in the center of the door assembly to provide flat field calibration images, spectral filters between the imaging system and the FPA to accurately select the requested spectral band, and linear polarizer to distinguish features of the solar corona.

The calibration campaign is conducted during the month of September 2021 at INAF calibration facility called OPSys (Optical Payload System calibration facility).

4.1 Calibration facility

The calibration facility was developed by INAF at ALTEC premises in Torino, Italy. The facility was initially designed for the calibration of METIS instrument, on-board the Solar Orbiter payload.

The OPSys facility is described in detail in [9] and is shown below in Figure 19.

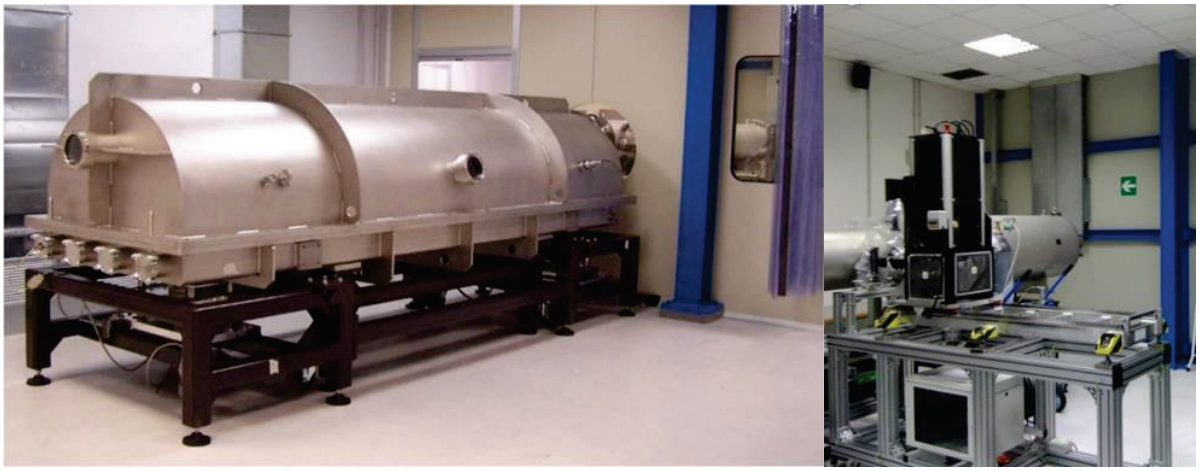

Figure 19. Vacuum chamber (left) and Sun Simulator Source (right) at INAF

The OPSys facility includes a thermal vacuum chamber (Space Optics Calibration Chamber (SPOCC)) with a motorized bench in an ISO5 environment. An appendix is hosting a solar simulator in another room (ISO8). This solar simulator consists in an off-axis parabola and a powerful visible light source (Illumination System in Visible Light, ISVL). It is able to simulate an artificial bright object with the equivalent divergence of the sun at the distance of the earth (1 A.U.). The brightness of the ISVL source is equivalent to $1/6^{th}$ of the sun brightness.

4.2 Calibration campaign

One of the main calibration phase of the campaign aims to characterize the radiometric properties of the APISSC FM instrument. Several steps are defined to perform this calibration.

First, an external flat field panel is used to perform flat field images with the instrument for all channels and with several integration times in air and at ambient temperature. The radiance of the flat field panel is measured and monitored, and the outputs of this test are reference flat field images of the instrument itself. For that test, the door is open and the HDD is not used. Figure 20 below illustrates the configuration where the FM instrument is located on the SPOCC chamber test bench looking at the flat field panel.

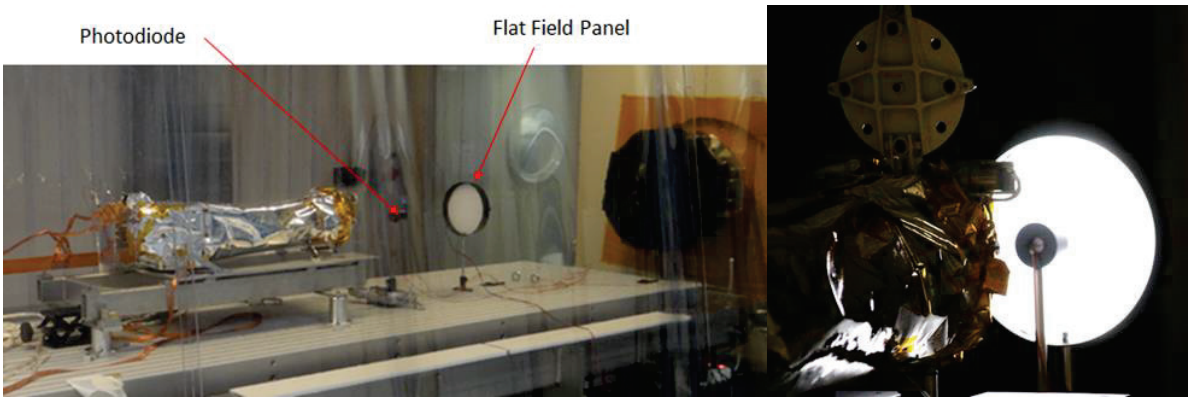

Figure 20. Setup configuration for flat field characterisation in air

The radiometric flat field reference images are quickly verified and the radiometric calibration of the HDD follows. For this calibration, several environmental radiometric tests are conducted. The door is closed and the sun simulator is used as depicted in Figure 21 below.

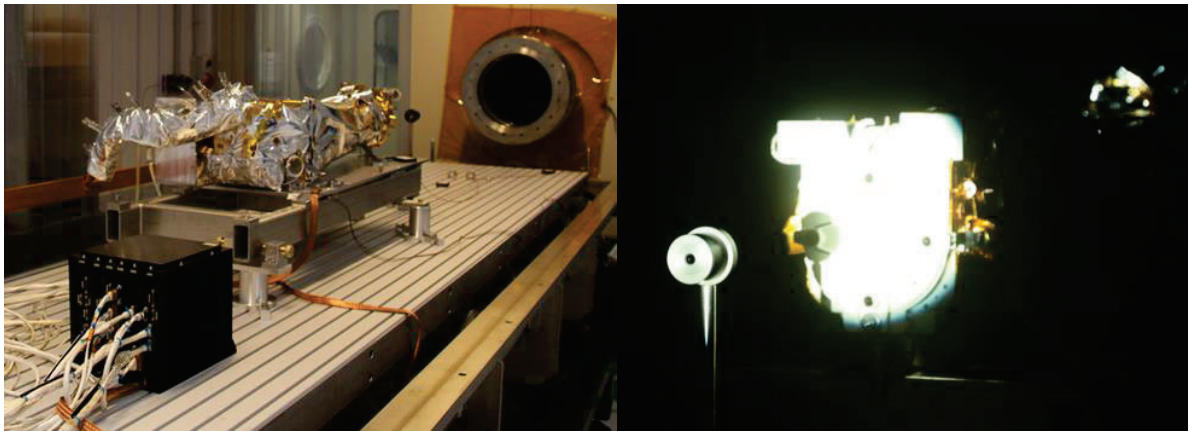

Figure 21. Setup configuration for flat field characterisation in vacuum (CI diffuser calibration)

A first reference test is made in air and at ambient temperature. The acquired images will be compared to the reference flat field images under the exact same environmental conditions. The sun simulator radiance is also known and monitored and the only difference is the use of the HDD diffuser instead of the external flat field panel.

After that, the SPOCC chamber is closed and 3 operational calibrations are performed under vacuum. For the first one, the FM instrument is heated up to 35°C with the help of internal heaters and calibration images are made with different integration times for all channels in light and dark conditions. This configuration is matching the condition of the alignment and performance tests performed during the FM test campaign at CSL. The instrument is in operational conditions and the imaging performances are known and confirmed.

Two additional calibration sequences are performed with a cooling down of the FPA temperature. Indeed, the detector assembly is featuring a CMOS detector which is designed to be cooled down to a temperature close to -30°C to exhibit its best radiometric performances. The cooling is designed to be passively performed by a radiator assembly linked to the detector, seeing a maximum of deep space temperature during the mission. Two operational temperature limits are driving these additional calibration sequences and were estimated during thermal analysis of the instrument.

A last calibration verification case is performed with the instrument in environmental condition corresponding to the hot in-orbit calibration phase where the instrument is not in the nominal observation environment: the CI temperature is estimated to increase up to +50°C due to the fact that the instrument is directly looking at the sun without being protected by the external occulter spacecraft.

In the end, the full HDD radiometric calibration sequence is the following:

1. Air, CI at room temperature (RT), FPA at RT (comparison case with flat field panel)
2. Vacuum, CI at +35°C, FPA not regulated (CI in operational condition – nominal imaging performance)
3. Vacuum, CI at +35°C, FPA at -13°C (Hot Operational temperature case)
4. Vacuum, CI at +35°C, FPA at -35°C (Cold Operational temperature case)
5. Vacuum, CI at +50°C, FPA at -13°C (Hot Calibration case – degraded imaging performances)

A programmatic constraint linked to the calibration facility imposed each calibration sequence to last a maximum of 6 hours in order to fit the sequence in one working day comprising the time needed for thermal stabilization of the instrument and detector. The acquisition sequence is thus carefully established to provide a maximum of useful images during this time period. A real-time verification of the images is implemented to quickly react in case of wrong behavior and to perform quick pre-validation of the acquired data.

The second important phase consisted in the calibration of the polarization performance of the instrument. To do that, the same flat-field setup as the first radiometric calibration in air is used. A rotating linear pre-polarizer is inserted between the flat field panel and the instrument to select a known linear orientation of the flat field illumination. This pre-polarizer is then rotated around the optical axis while images are acquired using the 3 linearly-polarized channels of ASPIICS. Figure 22 below illustrates the setup configuration.

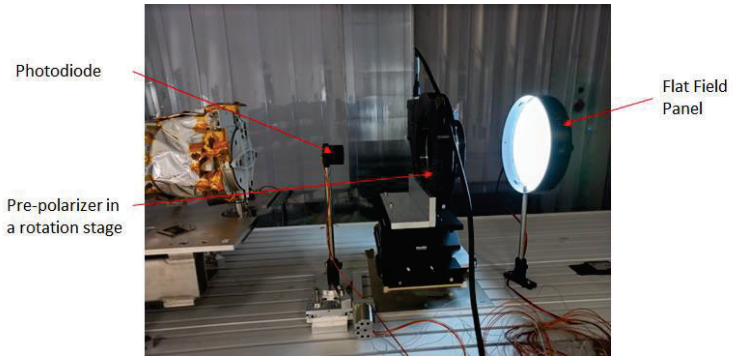

Figure 22. Setup configuration for polarization calibration

Finally, the spectral calibration mostly consisted in a validation of the spectral performance model of the instrument. Using the sun simulator, images of a tilted sun are acquired thought ASPIICS FM instrument for each spectral channel. For these measurements, an optical density is added after the source due to its high brightness. Additionally, specific spectral filters are also used to select in-band or out of band spectral range. The radiance of the source is known and monitored, and the spectral transmission of the optical density and filters are also previously characterized. The resulting relative irradiance between in-band and out of band measurements is compared to the spectral and radiometric model of the FM instrument constructed using measurements made at all FM subsystems level.

4.3 Results

All the needed calibration data are successfully acquired during the campaign and provided to the science team for further calibration processing and data reduction. Table 3 below shows a set of acquired flat field images with the HDD diffuser in vacuum and with the CI at operational temperature (sequence #2).

Table 3. CI Flat field images for all channel, under vacuum and operational conditions

		
WBF, IT 5s	POL1, IT 10s	POL2, IT 10s
		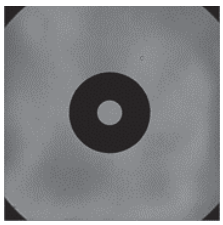
POL3, IT 10s	Fe, IT 150s	He, IT 50s

Some of the acquired data are however useful to verify high-level requirements for the FM instrument final acceptance. These results are briefly presented below in this chapter.

A radiometric performance was extracted during the calibration to verify a high level requirement on the instrument signal-to-noise ratio (SNR). This verification consists in the processing of flat field reference images which where made for each channel under the same illumination and environment. In these conditions, the SNR per pixel can be evaluated as the ratio between the average value per pixel of the corrected image and the standard deviation of the same pixel value over the number of acquisitions following equation (3) below:

$$SNR_{i,j} = \frac{mean\left(Is_{i,j} - Idark_{i,j}\right)}{std\left(Is_{i,j} - Idark_{i,j}\right)}$$

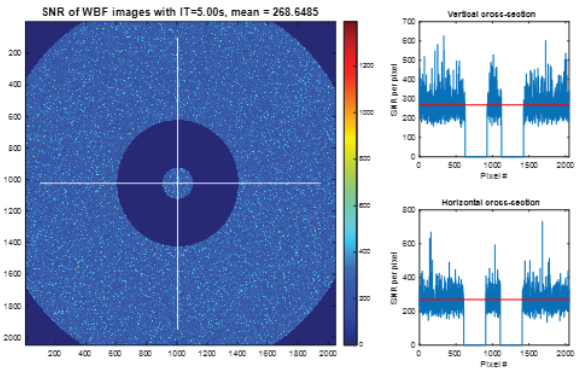

Figure 23. SNR per pixel computation

Figure 23 above illustrates the image processing result producing the SNR estimation per pixel on the whole detector useful region and Figure 24 below shows the assessed SNR versus integration time curves. The high level requirement of SNR >20 is reached and verified for each channel.

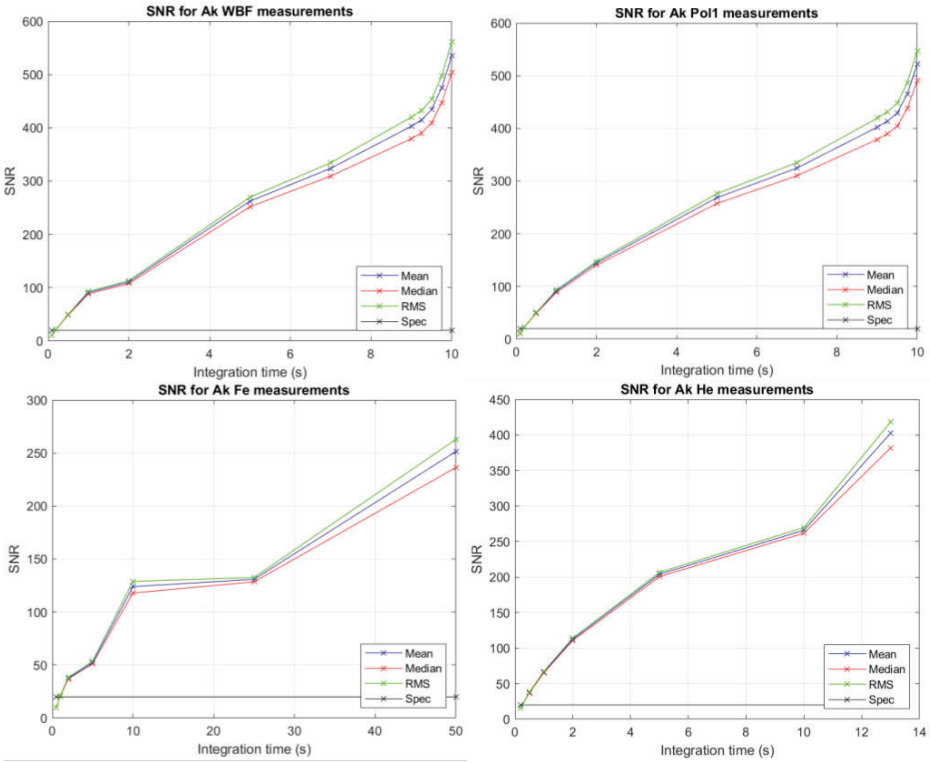

Figure 24: SNR assessment for 4 channels of ASPIICS

The other high-level requirement that can be verified concerns the ability to perform polarimetric images along three different linear directions, each separated by 60°. In order to verify this performance, the polarization calibration images are used to retrieve the Malus curve of each polarized channel. Table 4 below shows a flat field acquisition for each of the three channels for one orientation of the pre-polarizer.

Table 4. Polarization calibration images for 3 channels and one orientation of the pre-polarizer

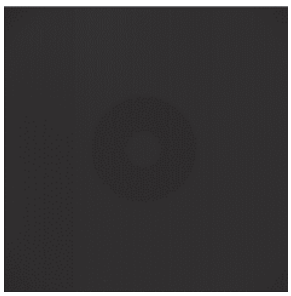	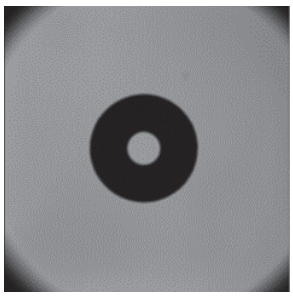	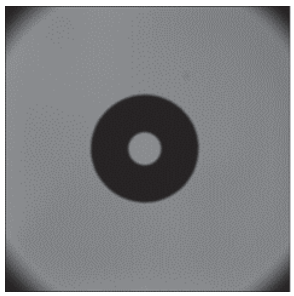
POL1, IT 2.5s, pre-pol 0°	POL2, IT 2.5s, pre-pol 0°	POL3, IT 2.5s, pre-pol 0°

The flat field images of all three channels were corrected of dark current and offset (dark images subtraction), averaged over all acquisitions and processed to extract the individual Malus curves as presented in Figure 25 below.

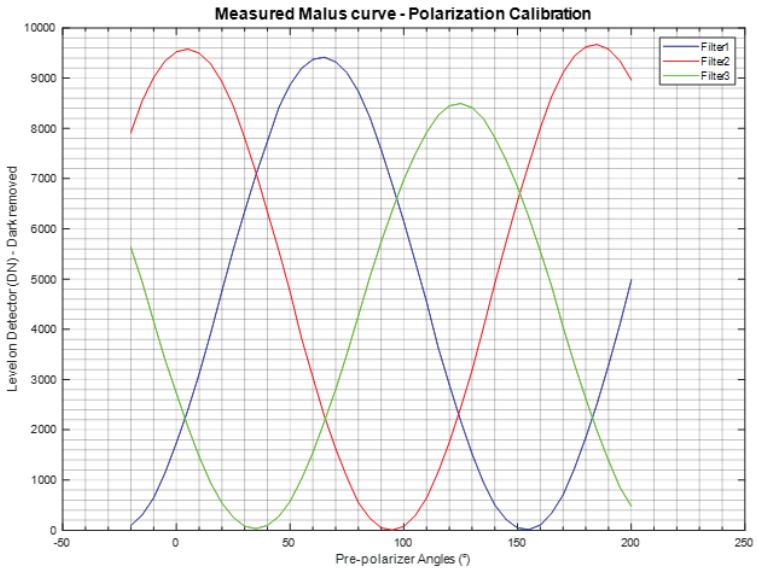

Figure 25. Experimental malus curve retrieval (3 polarizers)

Finally a mathematical fitting of the experimental curves with the theoretical Malus equation gives the final assessment of the polarized channel relative orientation as shown in Table 5 below.

Table 5. Polarizers relative orientation verification

Polarizers relative orientation						
	Pol1	**Pol2**	**Pol3**	**Pol1-Pol3**	**Pol1-Pol2**	**Pol2-Pol3**
θ_0 (°)	64.11	4.43	-55.56	119.67	59.68	59.99
Sigma (95%)	0.15	0.11	0.13	0.28	0.26	0.24

5 CONCLUSION

As a conclusion, this paper presented a wide time-span of the ASPIICS instrument qualification, acceptance and calibration phase from an optical point of view.

The QM alignment and performance test campaign was successfully conducted between the end of the year 2019 and the beginning of the year 2020. During this campaign, CSL's ability to design, integrate and validate an alignment and performance test setup was demonstrated and confirmed. The QM instrument performances reached a level which proved to be better than expected. This is mainly due to the reliable alignment setup specifically designed for ASPIICS.

Following the QM campaign, the FM acceptance test campaign took place a bit less than a year after, between the end of 2020 and the beginning of 2021. During this campaign, the operational alignment of the FM instrument was successfully performed and the optical performance test demonstrated a full compliance with the expected requirements. Despite some changes in the facility, improvements were also brought to the procedure and setup providing additional verifications which confirmed the FM instrument optical performances, temperature and through-focus tolerances.

At last, the calibration campaign was also successful and took place at ALTEC premises in Torino where INAF' calibration facility "OPSys" provided the necessary environment and equipment. A full set of on-ground calibration data could be produced and will be used by the scientific team to calibrate the radiometric, spectral and polarimetric behavior of the instrument. This calibration campaign also served to validate some high-level requirements necessary to complete the acceptance review of the FM instrument.

The ASPIICS FM instrument is now delivered to ESA and will be integrated on the PROBA-3 payload platform to be subjected to further high level testing before the launch date, planned for June 2023.

To conclude this paper, Figure 26 below shows the QM instrument while integrated on the PROBA3 coronagraph spacecraft structural model at CSL, and the FM instrument now integrated on the CSC flight model at QINETIC after delivery.

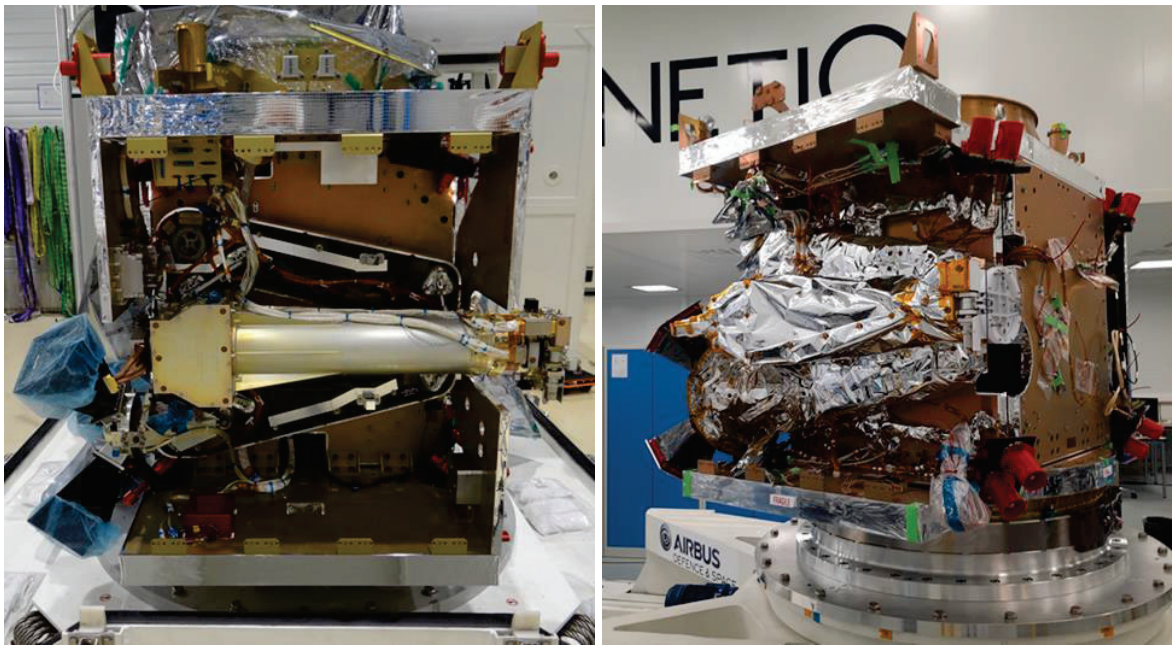

Figure 26: ASPIICS QM instrument integrated on the spacecraft structural model (left) and ASPIICS FM instrument integrated on the paylod FM model (right)

6 ACKNOWLEDGEMENTS

The ASPIICS project is developed under the ESA's General Support Technology Programme (GSTP) and the ESA's Prodex Programme thanks to the sponsorships of seven member states: Belgium, Poland, Romania, Italy, Ireland, Greece, and the Czech Republic.

REFERENCES

[1] Lamy, P., Vives, S., Damé, L., Koutchmy, S., "New perspectives in solar coronagraphy offered by formation flying: from PROBA-3 to Cosmic Vision", Proc. SPIE 7010, 70101H (2008)
[2] Lamy P.; Damé L.; Vives S.; Zhukov A., "ASPIICS: a giant coronagraph for the ESA/PROBA-3 Formation Flying Mission", SPIE Proc., Volume 7731, pp. 773118-773118-12 (2010)
[3] E. Renotte et al., "ASPIICS: An Externally Occulted Coronagraph for PROBA-3. Design Evolution", Space Telescope and Instrumentation, Montréal, SPIE 9143 - 87 (2014)
[4] E. Renotte et al., "Design status of ASPIICS, an externally occulted coronagraph for PROBA-3.", Optical Engineering and Applications, San Diego (USA), SPIE 9604 (2015)
[5] C. Galy et al., "Design and Modelisation of ASPIICS Optics", Optical Engineering and Applications, San Diego (USA), SPIE 9604 (2015)
[6] E. Renotte et al., "Recent achievements on ASPIICS, an externally occulted coronagraph for PROBA-3.", Astronomical Telescopes + Instrumentation, Edinburgh, SPIE 9904 – 121 (2016)
[7] D. Galano et al., "Development of ASPIICS: a coronagraph based on Proba-3 formation flying mission", Astronomical Telescopes + Instrumentation, Austin, SPIE 10698 (2018)
[8] C. Galy et al., "Straylight analysis on ASPIICS, PROBA-3 coronagraph", International Conference on Space Optics – ICSO 2018, Chania, Proc. SPIE 11180, 111802H (2019)
[9] G. Capobianco et al., "OPSys: optical payload systems facility for space instrumentation integration and calibration", International Conference on Space Optics – ICSO 2018, Chania, Proc. SPIE 11180, 111807M (2019)